Available online at www.sciencedirect.com
SCIENCE DIRECT®
Journal of Solid State Chemistry 174 (2003) 357–364
JOURNAL OF SOLID STATE CHEMISTRY
http://elsevier.com/locate/jssc

Phase transitions, structural changes and molecular motions in $[Zn(NH_3)_4](BF_4)_2$ studied by neutron scattering, X-ray powder diffraction and nuclear magnetic resonance

A. Migdał-Mikuli,[a,*] E. Mikuli,[a] Ł. Hetmańczyk,[a] I. Natkaniec,[b,c] K. Hołderna-Natkaniec,[d] and W. Łasocha[a]

[a] *Department of Chemical Physics, Faculty of Chemistry, Jagiellonian University, Ingardena 3, Kraków 30-060, Poland*
[b] *Frank Laboratory of Neutron Physics, JINR, Dubna 141980, Russia*
[c] *H. Niewodniczański Institute of Nuclear Physics, Radzikowskiego 152, Kraków 31-342, Poland*
[d] *A. Mickiewicz University, Institute of Physics, Umultowska 85, Poznań 61-606, Poland*

Received 25 November 2002; received in revised form 8 April 2003; accepted 26 April 2003

Abstract

Nuclear magnetic resonance (^{1}H NMR and ^{19}F NMR) measurements performed at 90–295 K, inelastic incoherent neutron scattering (IINS) spectra and neutron powder diffraction (NPD) patterns registered at 22–190 K, and X-ray powder diffraction (XRPD) measurements performed at 86–293 K, provided evidence that the crystal of $[Zn(NH_3)_4](BF_4)_2$ has four solid phases. The phase transitions occurring at: $T_{C3} = 101$ K, $T_{C2} = 117$ K and $T_{C1} = 178$ K, as were detected earlier by differential scanning calorimetry (DSC), were connected on one hand only with an insignificant change in the crystal structure and on the other hand with a drastic change in the speed of the anisotropic, uniaxial reorientational motions of the NH_3 ligands and BF_4^- anions (at T_{C3} and at T_{C2}) and with the dynamical orientational order–disorder process ("tumbling") of tetrahedral $[Zn(NH_3)_4]^{2+}$ and BF_4^- ions (at T_{C1}). The crystal structure of $[Zn(NH_3)_4](BF_4)_2$ at room temperature was determined by XRPD as orthorhombic, space group *Pnma* (No. 62), $a = 10.523$ Å, $b = 7.892$ Å, $c = 13.354$ Å and $Z = 4$. Unfortunately, it was not possible to determine the structure of the intermediate and the low-temperature phase. However, we registered the change of the lattice parameters and unit cell volume as a function of temperature and we can observe only a small deviation from near linear dependence of these parameters upon temperature in the vicinity of the T_{C1} phase transition.

Keywords: Tetraamminezinc(II) tetrafluoroborate; Phase transitions; Structural changes; Molecular motions

1. Introduction

The phase polymorphism and the connection of the phase transitions with structural changes and molecular motions in crystalline compounds of the type: $[M(NH_3)_6]X_2$, where M = Mg, Ni and $X = ClO_4$, BF_4, NO_3, was the main subject of many investigations by various methods (see, for example, Ref. [1] and the papers cited therein). It seems quite interesting to extend similar investigations also to the compounds of the type $[M(NH_3)_4]X_2$.

The polymorphism of $[Zn(NH_3)_4](BF_4)_2$ has been studied by Migdał-Mikuli et al. [2] with differential scanning calorimetry (DSC) and Fourier transform far-infrared spectroscopy (FT-FIR) measurements. The DSC measurements in the temperature range of 95–298 K detected three phase transitions at the following temperatures: $T_{C1} = 178$ K, $T_{C2} = 117$ K and $T_{C3} = 101$ K. The characteristic changes detected in the FT-FIR spectra in the temperature range of 25–298 K confirm the existence of four solid phases as deducted from the DSC measurements.

So far, no data have been available about the crystal structure of $[Zn(NH_3)_4](BF_4)_2$. However, we know that it is not isostructural with $[Zn(NH_3)_4](ClO_4)_2$ which has a cubic structure [3,4]. Our results of X-ray investigations (XRDP) of the crystal structure of $[Zn(NH_3)_4](BF_4)_2$ in the room temperature (RT) phase are presented in Chapter 3 of this paper. According to

*Corresponding author. Fax: +48-12-634-0515.
E-mail address: migdalmi@chemia.uj.edu.pl (A. Migdał-Mikuli).

0022-4596/03/$ - see front matter © 2003 Elsevier Inc. All rights reserved.
doi:10.1016/S0022-4596(03)00237-8

Kůtek [5], the chemical composition of the investigated compound is stable up to ca. 520 K.

The aim of the present study was to characterize the differences between the different phases formed by the title compound and to find its connection with reorientational motions of the NH_3 ligands and the BF_4^- anions, as well as with changes in the crystal structure. We also present the crystal structure of the RT phase of the title compound. Unfortunately, it was not possible to determine the structure of the intermediate and the low-temperature phase. However, we registered the change of the lattice parameters of the RT phase as a function of temperature. The investigations were performed with inelastic incoherent neutron scattering (IINS), neutron powder diffraction (NPD), X-ray powder diffraction (XRPD) and nuclear magnetic resonance (^{1}H NMR and ^{19}F NMR). A comparison with the results obtained earlier by DSC and FT-FIR [2] was also made.

2. Experimental

The sample of the title compound investigated in the present study was employed earlier in the DSC and FT-FIR studies [2], and the details of synthesis and chemical analysis of the title compound were also described in that paper.

The XRPD data were collected on a Philips X'Pert (PW1710) powder diffractometer, using graphite monochromatized Cu$K\alpha$ radiation. The details of RT measurement are listed in Table 1. For low-temperature measurements, an Anton Paar TTK 2-HC camera was used. The diffraction patterns were collected in the 2Θ range of 10–55°, with the scan step of 0.02° and the step time of 1 s, while the sample was heated up from 86 K to the RT. The sample was protected against decomposition by Nujol.

The NPD and IINS spectra were measured simultaneously using the time-of-flight method in the NERA spectrometer [6] in the high-flux pulsed reactor IBR-2 in Dubna (Russia). The sample was mounted into a thin-wall aluminum container, $(140 \times 60 \times 1)\,mm^3$, at RT. The sample holder was then placed in a top-loaded cryostat cooled with a helium refrigerator. The temperature of the sample could be changed within the range 20–300 K and stabilized with ± 0.5 K accuracy at any chosen value. The energy resolution of the NERA-PR spectrometer amounts to ca. 3% for the IINS spectra in the range 100–1000 cm^{-1}. The spectral width of the elastic peak at 4.2 Å equals ca. 5 cm^{-1}. The IINS and the NPD measurements were made for several scattering angles. The final IINS spectra were obtained by summing up the data taken from all 15 detectors, which cover scattering angles from 20° to 160°. In the case of the NPD, different angles were used to record the chosen ranges of the lattice spacing d_{hkl} at an appropriate resolution. It should be stressed that because the investigated compound contains 2 boron and 12 hydrogen atoms per formula unit, the NPD spectra had a weak intensity due to strong neutron absorption by boron atoms and were recorded on a relatively high incoherent background caused by the scattering of hydrogen atoms. For this reason, their interpretation is only qualitative, but it was very useful for the identification of particular phases.

The apparatus for the proton magnetic resonance (^{1}H NMR) and fluorine magnetic resonance (^{19}F NMR) measurements was a 25 MHz laboratory-made instrument operating in the double modulation system.

Table 1
Crystallographic data

Crystal data, measurements	Powder diffraction, Philips X'Pert, Bragg–Brentano geometry
Material and its color	Polycrystalline, white
Empirical formula	$[Zn(NH_3)_4](BF_4)_2$
Formula weight	307.12 g/mol
Crystal system	Orthorhombic
Space group	*Pnma* (No 62)
Unit cell dimensions	$a = 10.523(2)$ Å, $b = 7.892(1)$ Å, $c = 13.354(2)$ Å
Volume	1109.0(2) $Å^3$
Z	4
Calculated density	1.8395 g/cm^3
F_{30}*	69.16 (0.00923, 47)
M_{30}**	28.46 (0.00006, 47)
Wavelength	$\lambda = 1.54178$ Å (Cu $K\bar{\alpha}$)
Temperature	295 K {86, 110,140, 150, 160, 200, 225, 250, 293 K}
2Θ range for data collection	10–95° {10–55°}
Scan step size	0.020° {0.020°}
Scan step time	12 s {1 s}
Number of contributing reflections	552
Refinement method	X-ray Rietveld System XRS-82
No. of parameters refined	34
Final R_F and R_{wp} factors	17.7% and 13.0%
Texture correction formula	exp(Gcos2α)
Preferred orientation function, vector and factor G	[101] and −0.27

Note: The parameters for the low-temperature measurements are in parentheses: { }.

*P.M. de Wolf, A definition of the indexing figure of merit M_{20}, J. Appl. Crystallogr. 5 (1972) 243.

**G.S. Smith, R.L. Snyder, FN: a criterion for rating powder diffraction patterns and evaluating the reliability of powder-pattern indexing, J. Appl. Crystallogr. 12 (1979) 60.

3. Results and discussion

3.1. Crystal structure of $[Zn(NH_3)_4](BF_4)_2$ at RT

The structure of $[Zn(NH_3)_4](BF_4)_2$ at RT was solved from powder diffraction data using the EXPO package

[7] and the XRS-82 Rietveld Refinement system [8,9]. During the measurement, the sample was protected against hydrolysis and decomposition by Nujol. The diffraction pattern was indexed in the orthorhombic system by a program written by Visser [10]. After refinement of the lattice constants by means of the PROSZKI system [11], the space group *Pnma* was found by systematic absences analysis. The initial model of the crystal structure was based on EXPO results and supported by the crystal structure of similar compounds $[Zn(NH_3)_4]I_2$ and $[Zn(NH_3)_4]Br_2$ [12,13] and completed by the Fourier method using XRS-82. Both Zn and B atoms are tetrahedrally coordinated by four N and F atoms, respectively. Rather high values of thermal displacement parameters for B and F atoms and weak electron density maxima which could be located around Zn and B atoms, may indicate some kind of rapid reorientation, orientational disorder or high-amplitude vibrational motion of BF_4^- anions. However, introducing more than four ligands into $[Zn(NH_3)_4]^{2+}$ and BF_4^- ions with partial occupancy did not lower *R* factors significantly, but causes instability of refinement. So, the atomic positions listed in Table 2 presented an "averaged" structure model without disorder. The crystal data for $[Zn(NH_3)_4](BF_4)_2$ and measurement details are presented in Table 1. The coordinates of atoms (with the exception of hydrogen), thermal displacement parameters and the selected bond lengths (Å) and angles (°) are listed in Table 2. Fig. 1 presents a view of the unit cell and the atom numbering used. Fig. 2 shows calculated, observed and difference Rietveld profiles of $[Zn(NH_3)_4](BF_4)_2$ at RT.

Table 2
Coordinates of atoms (with exception of hydrogen), thermal parameters, atomic distances and bond angles

Atom	*x*	*y*	*z*	U^*
Zn	0.744(1)	0.25	0.4067(9)	0.033(3)
N1	0.553(2)	0.25	0.424(3)	0.13(2)
N2	0.828(4)	0.25	0.542(2)	0.1278
N3	0.797(2)	0.042(2)	0.330(1)	0.1278
B1	0.330(2)	0.25	0.414(2)	0.3(3)
B2	0.488(2)	0.25	0.806(2)	0.3407
F1	0.375(5)	0.25	0.514(3)	0.170(6)
F2	0.197(3)	0.25	0.414(5)	0.1704
F3	0.377(3)	0.099(2)	0.363(2)	0.1704
F11	0.362(3)	0.25	0.800(2)	0.21(2)
F12	0.541(4)	0.25	0.710(3)	0.2129
F13	0.527(2)	0.390(2)	0.856(2)	0.2129
Distances (Å)	Zn–N1	2.02(3)		
	Zn–N2	2.01(3)		
	Zn–N3	2.01(2)		
	B1–F1	1.42(5)		
	B1–F2	1.41(3)		
	B1–F3	1.46(3)		
	B2–F11	1.34(4)		
	B2–F12	1.41(4)		
	B2–F13	1.35(3)		
Mean angles (deg)	⟨N–Zn–N⟩	109.5±1.5		
	⟨F–B1–F⟩	109.5±3.0		
	⟨F–B2–F⟩	109.5±2.7		

Note: The e.s.d. of the last significant digit is given in parentheses.
*The *U* values without e.s.d. were constrained to the equal to proceeding one.

3.2. Phase-transition measurements

The X-ray diffraction patterns for the polycrystalline $[Zn(NH_3)_4](BF_4)_2$, were registered at 86, 110, 140, 150, 160, 200, 225, 250 and 293 K. No distinct differences were observed between all these diffraction patterns, which means that the space group *Pnma* (No. 62) is the same for all four phases of $[Zn(NH_3)_4](BF_4)_2$. The refinement was done using Rietica software package [14]. We divided the refinement process into two steps. At first the background was fitted; then using the Le Bail method [15] the full profile matching was performed. The background was fitted in an arbitrary way by linear interpolation between ca. 30 points because of the presence of an amorphous hump in the diffraction pattern resulting from Nujol. During the full-profile matching (step two), the refined lattice parameters (*a*, *b*, *c*) were obtained. The initial model for refinement was based on the data obtained for $[Zn(NH_3)_4](BF_4)_2$ at RT (see Section 3.1). Fig. 3 presents the temperature dependence of the lattice parameters (*a*, *b*, *c*) and the volume (*V*) of the title compound's unit cell. No drastic changes can be observed in these dependences at the T_{C3}

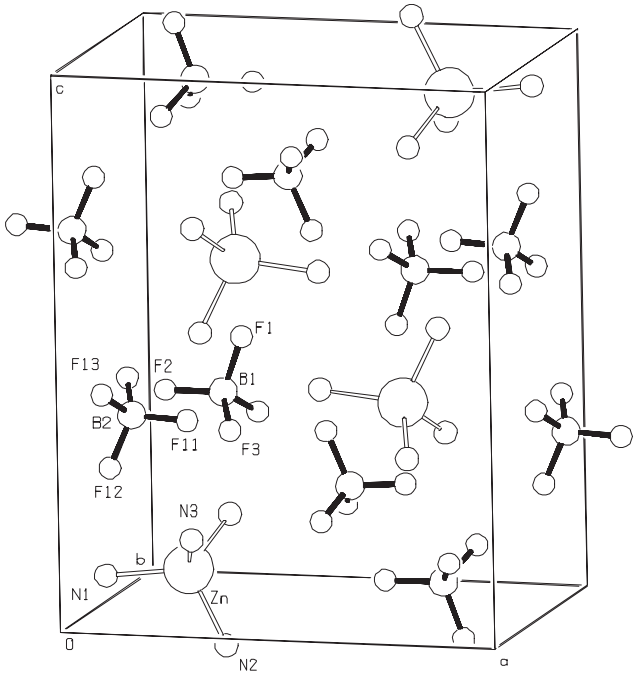

Fig. 1. Unit cell of $[Zn(NH_3)_4](BF_4)_2$ and atoms numbering used.

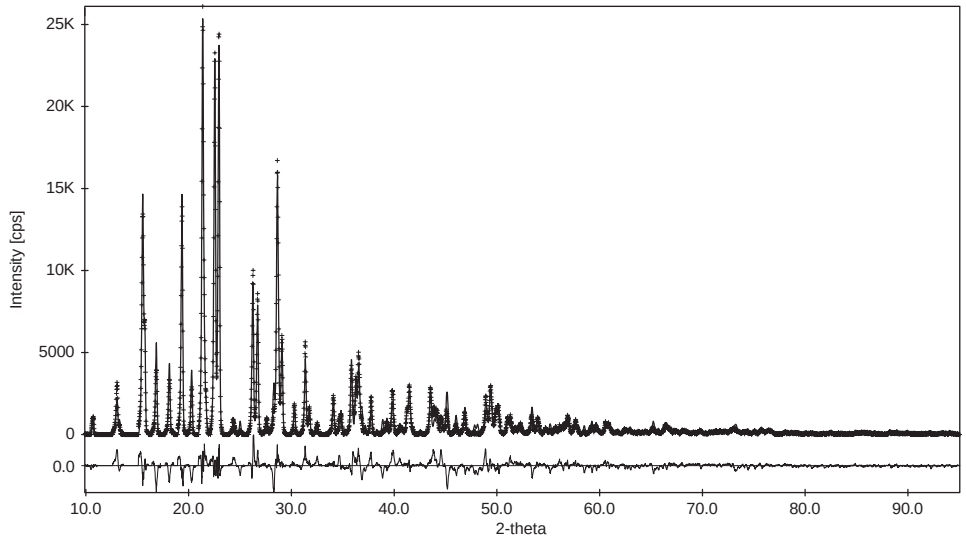

Fig. 2. Calculated (---), observed (+ + +) and difference (lower ----) Rietveld profiles of $[Zn(NH_3)_4](BF_4)_2$ at RT.

and T_{C2} phase-transition regions. We can observe only a small deviation from near-linear dependence of the lattice parameters and the volume upon temperature in the vicinity of the T_{C1} phase transition. In terms of X-ray measurements, it means that only small structural changes take place in the T_{C1} phase transition.

The neutron diffraction patterns for the polycrystalline $[Zn(NH_3)_4](BF_4)_2$, registered while the sample was heated up at seven chosen temperatures of measurement, are shown for two scattering angles in Fig. 4. There are some small but well noticeable differences between the NPD patterns obtained for particular phases. Namely, very small differences can be noticed between the diffraction patterns obtained at 70 and 102 K. They can be well seen in the case of two reflexes located at d_{hkl} spacing, equal to 4.35 and 4.45 Å (see Fig. 4a) and 3.05 and 3.20 Å (see Fig. 4b). These differences can be connected with a very small change in the crystal structure and can be related to the phase transition which was registered by DSC [2] at $T_{C3} = 101$ K. The biggest differences can be observed between the patterns registered at 112 and 125 K. They can be easily visible in the case of three reflexes located on NPD patterns at d_{hkl} spacing equal to 3.75, 4.40 and 4.75 Å (see Fig. 4a), and 3.00, 3.07 and 3.35 Å (see Fig. 4b). These differences are undoubtedly connected with the very small change of the crystal structure, but they can be interpreted as an evidence of the next phase transition. A good correlation with the phase-transition temperature, as registered in the DSC experiment [2] at $T_{C2} = 117$ K, is obvious. There are only very small differences between the patterns registered at 170 and 190 K. They can be seen only in the case of the reflexes located at d_{hkl} equal to 2.81 and 3.01 Å (see Fig. 4b). It indicates that the phase transition detected by DSC [2] at $T_{C1} = 178$ K is not connected with the change of the crystal structure, at least from the point of view of neutron diffraction method.

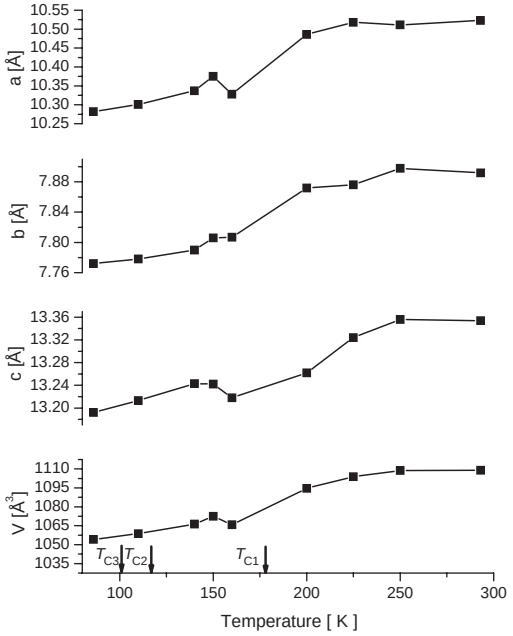

Fig. 3. Temperature dependence of the lattice parameters (a, b, c) and volume (V) of the unit cell of $[Zn(NH_3)_4](BF_4)_2$.

The time-of-flight IINS spectra of $[Zn(NH_3)_4](BF_4)_2$ against the neutron wavelength scale, registered simultaneously with the NPD patterns, for seven chosen temperatures of measurements are presented in Fig. 5. Noticeable differences between the IINS spectra at the low wavelength values can be seen for the spectra that were registered at temperatures of 70 and 102 K, 112 and 125 K, and 170 and 190 K. These changes can be linked to the occurrence of the three phase transitions in the sample detected by DSC measurements [2].

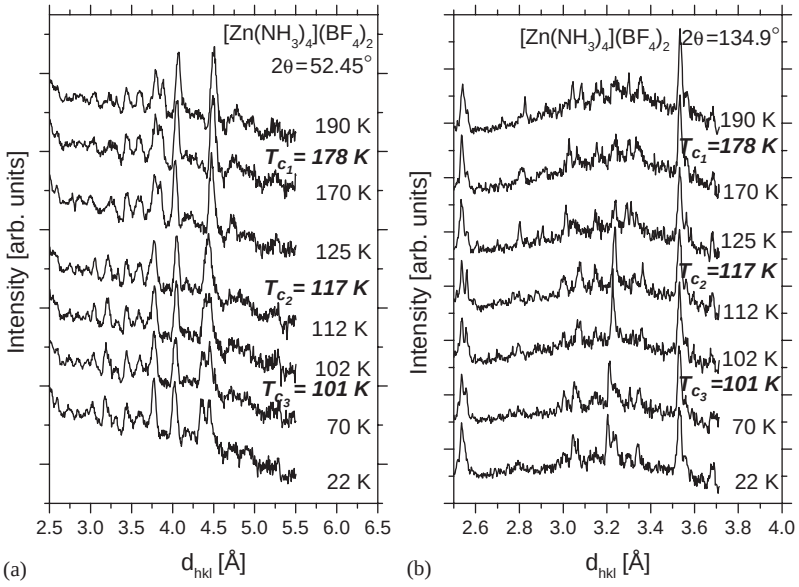

Fig. 4. The NPD patterns of $[Zn(NH_3)_4](BF_4)_2$ registered on heating the sample for seven chosen temperatures of measurement: (a) at scattering angle $2\theta = 52.45^\circ$ and (b) at scattering angle $2\theta = 134.90^\circ$.

In the IINS spectra presented in Fig. 5, one can also observe a distinct difference between the width of the elastic peak (centered at a wavelength of 4.3 Å) registered at the temperature below and above ca. 100 K. The elastic peak, registered at 102 K and also at higher temperatures, shows a distinct broadening, that is typical for dynamically orientationally disordered crystals [16]. Particularly, a quasielastic neutron scattering (QNS) component is very clearly visible left to the elastic peak. Given the energy resolution of the NERA spectrometer, this implies the occurrence of fast stochastic molecular motions. It is inferred that these are the picosecond reorientational 120° jumps of NH_3 molecules around their three-fold axis of symmetry. Such type of motion was earlier observed in many hexaamminemetal(II) compounds (see, for instance, Ref. [1] and the papers cited therein). On the other hand, the quasielastic broadening does not exist in the IINS spectra of the title compound at 70 and 22 K. This fact can be explained as evidence that at the phase transition to the low-temperature phase T_{C3}, all NH_3 ligands suddenly change the speed of their reorientational motion (e.g. the reorientational correlation time τ_R of the NH_3 ligands becomes longer than 10^{-10} s). During the heating of the title compound from the low-temperature phase IV to the intermediate phases III and II, the full-width at half-maximum (FWHM) of the QNS component of the elastic peak distinctly increases. Thus, we conclude that at T_{C3} and next at T_{C2} phase transitions, first at least a part and next the remainder NH_3 ligands, respectively, start their fast reorientation motion (with $\tau_R \ll 10^{-10}$ s). At the high-temperature phase I, all NH_3 ligands reorientate fast, probably in a picosecond scale.

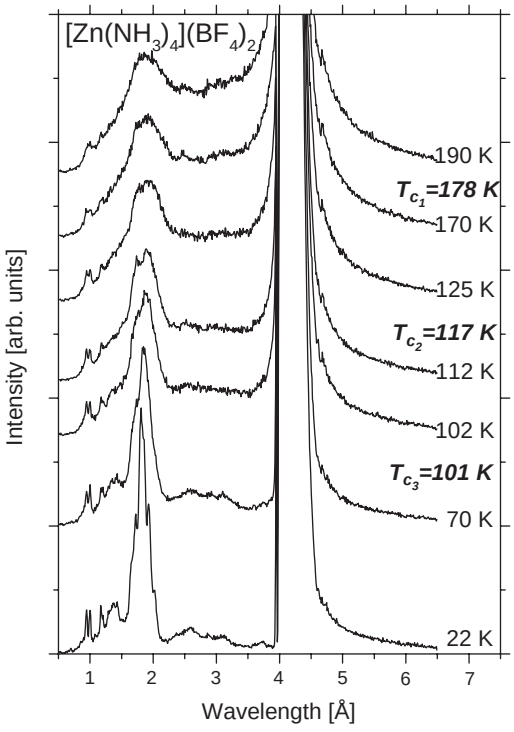

Fig. 5. The IINS spectra of $[Zn(NH_3)_4](BF_4)_2$ registered simultaneously with NPD patterns which were presented in Fig. 4.

The title compound was also subjected to ^1H NMR and ^{19}F NMR studies. The slope line width (δH) and the second moment (M_2) were determined from the NMR line derivative [17]. The measurements were performed on heating the sample. Fig. 6a shows the temperature dependence of the slope line width and the second moment of ^1H NMR line. At 90 K the second moment

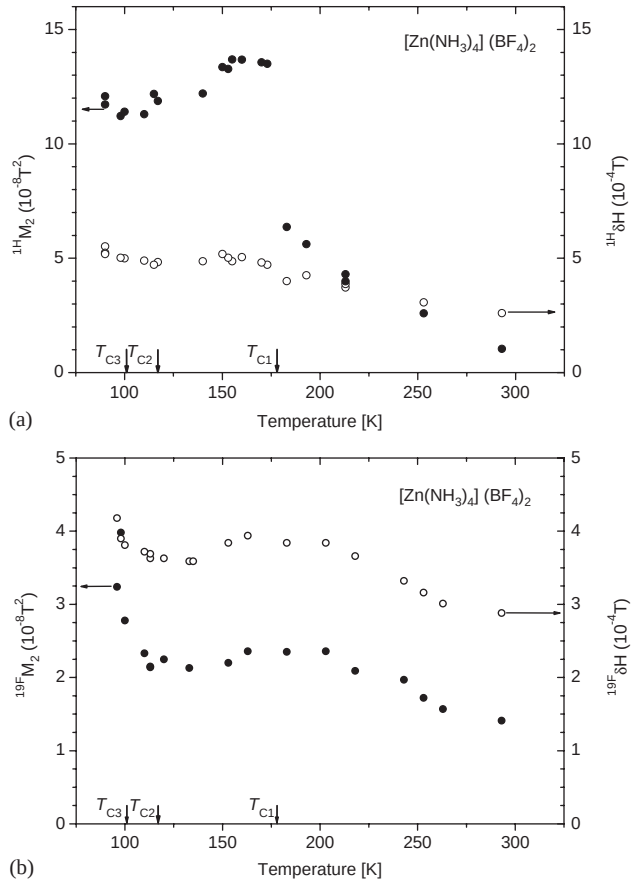

Fig. 6. Temperature dependence of the line width and second moment of ^{1}H NMR (a) and ^{19}F NMR (b) lines of $[Zn(NH_3)_4](BF_4)_2$.

takes the value of $13.0 \times 10^{-8}\,T^2$. No changes in δH and ^{1}H M_2 of ^{1}H NMR line were found in the vicinity of 101 and 117 K (T_{C3} and T_{C2}). When the temperature was increased to 178 K (T_{C1}), ^{1}H M_2 was almost constant, and at 178 K its value rapidly changed to $7.0 \times 10^{-8}\,T^2$. The abrupt ^{1}H M_2 transitions at ca. 178 K are apparently associated with the thermal phase transition T_{C1}. With temperature increasing to 300 K, ^{1}H M_2 smoothly decreases, approaching the value of $1.2 \times 10^{-8}\,T^2$. The width of the ^{1}H NMR line of $5 \times 10^{-4}\,T$ in temperatures 90–170 K continuously decreases to $2.5 \times 10^{-4}\,T$ on heating the sample from the phase-transition point T_{C1} to 300 K.

The second moment value for the rigid lattice was determined from the van Vleck formula [18]

$$M_2 = \frac{3}{5}\gamma_H^4\hbar^2 I(I+1)\frac{1}{N}\sum_{j,k}^{N} r_{H-H}^{-6} + \frac{4}{15}\gamma_S^4\hbar^2 S(S+1)\frac{1}{N}\sum_{j,k}^{N} r_{H-S'}^{-6}, \quad (1)$$

where I is the resonant spin, S the nonresonant spins, γ_H the gyromagnetic ratio of resonant spin, γ_S the gyromagnetic ratio of nonresonant spins, $r_{j,k}$ the internuclear distance in the whole sample and N the number of resonant spins in the molecule.

In order to calculate the so-called intramolecular contribution to the second moment M_2^{intra}, which is dominant, the practically assumed procedure was to sum up the inverse values of the internuclear distances between cation and anions lying in near neighborhood in an "isolated molecule" to the sixth power. The intermolecular contribution to the second moment M_2^{inter}, is calculated from Eq. (1) as a sum of the inverse values of the internuclear distances of neighbouring molecules to the sixth power, or from the relationship given in Ref. [19] for globular molecules. The total $M_2 = M_2^{intra} + M_2^{inter}$ is compared with the experimental value.

The methods for calculation of the rigid value of M_2 and the effects of various molecular reorientations are summarized in Refs. [19–21]. The second moment of the ^{1}H NMR line was calculated by taking into account the interactions between H–H, H–N and H–F nucleus, while the second moment of the ^{19}F NMR line was calculated by taking into regard the F–F, F–H, F–N interactions. Given the structural parameters from our X-ray diffraction study, and assuming that all N–H bond distances were of 1.00 Å and all the N–H bonds were tetrahedrally directed with respect to the Zn–N bonds [22,23], we find ^{1}H $M_2^{rigid} = 47.3 \times 10^{-8}\,T^2$, as a sum of 40.2, 2.2 and 3.7 (in $10^{-8}\,T^2$) from H–H, H–F and H–N intramolecular interactions, respectively, whereas the intermolecular contribution to ^{1}H M_2 takes the value of $1.2 \times 10^{-8}\,T^2$. The rotation about an axis making the angle $\gamma_{j,k}$ to the radius vector of a pair of the nuclei $r_{j,k}$ would reduce the intramolecular contribution of the pair interaction to the second moment according to the formula [17]

$$M_2^{rot} = M_2^{rigid}\left(\frac{3\cos^2\gamma_{j,k} - 1}{2}\right)^2. \quad (2)$$

The reorientations of four ammonia ligands about the three-fold symmetry axis Zn–N at frequencies higher than the ^{1}H NMR line width (in s^{-1}) reduce the second moment to $12.4 \times 10^{-8}\,T^2$, which is close to the value obtained at 90 K. The effect of the cation's anisotropic reorientations about its three-fold symmetry axis on ^{1}H M_2 is significant, and ^{1}H $M_2 = 6.3 \times 10^{-8}\,T^2$, which is close to the value observed at 180 K, (close to T_{C1}). It is generally known that, for the general molecular reorientation, the ^{1}H NMR second moment is of about $1 \times 10^{-8}\,T^2$, and such a value is observed at 300 K.

The analysis of the theoretical intramolecular contribution to the rigid lattice ^{19}F second moment was performed assuming the structure determined by X-ray diffraction study at RT. The intramolecular contributions to the second moment of ^{19}F NMR line coming from the interactions between the F–F, F–H and F–N

nuclei are 7.06, 5.9 · and 0.03 (in $10^{-8}\,T^2$), respectively, while the intermolecular contribution was $3.2\times10^{-8}\,T^2$, so the total ^{19}F M_2 value for the rigid lattice was $16.2\times10^{-8}\,T^2$.

The reorientations of both BF_4^- ions about the three-fold symmetry axis with a simultaneous reorientation of the cation reduced the value of ^{19}F M_2 to $2.37\times10^{-8}\,T^2$, which is observed in the temperature range from 125 to 200 K (see Fig. 6b). The X-ray data indicate different isotropic thermal parameters and different internal bond length. The onset of the isotropic tumbling of one BF_4^- group gave the second moment of $1.64\times10^{-8}\,T^2$, close to $1.4\times10^{-8}\,T^2$ determined at 300 K.

The analysis of the ^1H and ^{19}F NMR second moment values and the temperature dependence of the slope line width provides information on the molecular motion undergoing a change with the frequency of an order of NMR line width, i.e. $10^{-4}\,s^{-1}$. The temperature dependence of the NMR line-width is described by the BPP [24] formula:

$$(\delta H)^2 = B^2 + (C^2 - B^2)2/\pi\,\mathrm{arctg}(\alpha\gamma\delta H/2\pi\nu_c), \qquad (3)$$

where δH is the NMR line width at a temperature T (when $\delta H \sim \nu_c$), B, C the NMR line width determined for the high- and low-temperature plateau, for $\delta H \ll \nu_c$ or $\delta H \gg \nu_c$, respectively, α a constant of the order of 1, γ the gyromagnetic factor of resonant nucleus, ν_c the frequency of intramolecular reorientations described by the Arrhenius dependence: $\nu_c = \nu_0 \exp(-E_a/RT)$.

From formula (3), it is possible to calculate the activation energy E_a of the intramolecular reorientations taking place at frequencies of the order of the NMR line width. The activation energy of intramolecular reorientations can be also estimated to an accuracy of 20% from the approximate relation given by Waugh and Fedin [25]:

$$E_a \approx 37 T_p, \qquad (4)$$

where T_p is the temperature at the point corresponding to the line width value of $(B + C)/2$.

Taking into regard that the calculated second moment ^1H M_2 value for the rigid lattice structure in $[Zn(NH_3)_4](BF_4)_2$ is $47.3\times10^{-8}\,T^2$ and ^1H M_2 value calculated, taking into account the reorientation of all 4 NH_3 ligands around their three-fold symmetry axes is $12.4\times10^{-8}\,T^2$, it can be assumed that the ^1H NMR line width δH, determined at 100 K as $5\times10^{-4}\,T$, is related to the uniaxial reorientation of the NH_3 molecule.

Similar ^1H and ^{19}F NMR measurements were performed for $[Ni(NH_3)_6](BF_4)_2$ by Sagnowski et al. [26]. Calculated by these authors ^1H M_2 value for the rigid lattice of $[Ni(NH_3)_6](BF_4)_2$ is $47.74\times10^{-8}\,T^2$, but experimental value of this second moment at the liquid helium temperature was $34.16\times10^{-8}\,T^2$. Assuming that BF_4^- ions reorient isotropically and all the six NH_3 ligands rotate about their three-fold axes, calculated ^1H M_2 value is $16.07\times10^{-8}\,T^2$. Taking into account, additionally, the tumbling motion of $[Ni(NH_3)_6]^{2+}$ cations, the ^1H M_2 value decreases to $6.84\times10^{-8}\,T^2$ [26]. Experimental values of this second moment were 10.85×10^{-8} and $7.17\times10^{-8}\,T^2$ at 160–220 K and at RT, respectively [26].

The activation energy of the NH_3 reorientation in $[Zn(NH_3)_4](BF_4)_2$ may be estimated from the Waugh–Fedin formula (4) as lower than 3.4 kcal/mol, assuming that the process of hindered reorientation of the NH_3 ligands undergoes below 90 K. The activation energy of the NH_3 reorientation in $[Zn(NH_3)_4]I_2$ and $[Zn(NH_3)_4]Br_2$ estimated from QNS measurement [27] is close to 0.7 kcal/mol, while in $[Cd(NH_3)_6](BF_4)_2$, takes the value of 2.0 kcal/mol, determined from the temperature study of the spin-lattice relaxation time T_1 [28].

The line narrowing in the vicinity of 180 K is associated with the anisotropic reorientation of the $[Zn(NH_3)_4]^{2+}$ cations, (as suggested by the NMR second moment analysis). Just above 180 K, the onset of the isotropic reorientation (tumbling) was observed. The activation energy for the isotropic cation reorientation estimated from the Waugh–Fedin formula is $E_a \approx 7.4$ kcal/mol, and 6.8 kcal/mol from the BPP formula (3), which is close (within the 20% error range) to the activation energy of 6.6 kcal/mol, determined in the temperature dependence of the spin-lattice relaxation time study of $[Cd(NH_3)_6]^{2+}$ reorientation [28].

In the ^{19}F NMR spectrum, a narrowing of δH and ^{19}F M_2 of the resonance line was observed (see Fig. 6b) in the temperatures from 90 to 100 K and from 178 to 300 K, which indicates the onset of anisotropic and isotropic BF_4^- anion reorientations, respectively. The activation energy for both reorientations of BF_4^- were estimated from the Waugh–Fedin formula as $E_a \approx 3.3$ and 9.2 kcal/mol.

4. Conclusions

1. The structure of $[Zn(NH_3)_4](BF_4)_2$ at room temperature (phase I) was determined from powdered diffraction data. The compound crystallized in an orthorhombic system, space group *Pnma* (No. 62), with $a = 10.523$ Å, $b = 7.892$ Å, $c = 13.354$ Å and $Z = 4$. High values of the thermal displacement parameters for B and F atoms indicate rapid reorientation or orientational disorder of BF_4^- anions.
2. The orientational order–disorder and structural phase transitions were observed in the neutron scattering, X-ray and NMR measurements, while the sample was being heated up. The phase-transition temperatures detected by DSC [2] at $T_{C1} = 178$ K, $T_{C2} = 117$ K and at $T_{C3} = 101$ K are well consistent

with changes observed in neutron scattering, X-ray diffraction and NMR data. Thus, the $[Zn(NH_3)_4](BF_4)_2$ has four solid phases in the temperature range of 20–300 K: phase I above 178 K, phase II from 178 to 117 K, phase III from 117 to 101 K, and finally phase IV, below 101 K.

3. At the phase transition from the low-temperature phase IV to phase III at T_{C3}, the speed of uniaxial reorientational motion, at least of a part of the NH_3 ligands, changes drastically (their reorientational correlation time τ_R became shorter than 10^{-10} s). Additionally, the slow ($\tau_R \approx 10^{-4}$ s) anisotropic (uniaxial) reorientation of BF_4^- anions is set in motion too. At the phase transition from phase III to phase II at T_{C2}, fast reorientation ($\tau_R \approx 10^{-10} - 10^{-12}$ s) of the remainder NH_3 ligands is set in motion too. At the phase transition from the intermediate (phase II) to the high-temperature phase (phase I) at T_{C1}, the $[Zn(NH_3)_4]^{2+}$ cations start their slow ($\tau_R \approx 10^{-4}$ s) isotropic reorientation (tumbling) and the BF_4^- anions start their fast isotropic reorientation as well. Thus, the general dynamical reorientational disorder is observed in the title compound at room temperature phase.

Acknowledgments

Technical help of M.Sc. M. Michalec and M.Sc. M. Grzywa with low-temperature X-ray measurements is kindly acknowledged.

References

[1] J.M. Janik, J.A. Janik, A. Migdał-Mikuli, E. Mikuli, K. Otnes, Physica B 168 (1991) 45.
[2] A. Migdał-Mikuli, E. Mikuli, Ł. Hetmańczyk, E. Ściesińska, J. Ściesiński, S. Wróbel, N. Górska, J. Mol. Struct. 596 (2001) 123.
[3] A.M. Dezor, K. Kędzia, Proceedings of the Conference of RAMIS-79 UAM, Poznań, Poland, 1979.
[4] H. Hillebrecht, G. Thiele, A. Koppenhöfer, H. Vahrenkamp, Z. Naturforsch. 49b (1994) 1163.
[5] F. Kůtek, Coll. Czechoslov. Chem. Commun. 32 (1976) 2353.
[6] I. Natkaniec, S.I. Bragin, J. Brańkowski, J. Mayer, in: Proceedings of the ICANS XII Meeting, Abington, 1993, RAL Report 94-025, Vol. I, 1994, pp. 89–96.
[7] A. Altomare, M.C. Burla, G. Cascarano, C. Giacovazzo, A. Guagliardi, A.G.G. Moliterni, G. Polidori, J. Appl. Crystallogr. 32 (1999) 339.
[8] Ch. Baerlocher, XRS-82, The X-ray Rietveld System, Institut f. Kristallographie, ETH, Zürich, Switzerland, 1992.
[9] D. Mucha, W. Łasocha, J. Appl. Crystallogr. 27 (1994) 201.
[10] J.W. Visser, J. Appl. Crystallogr. 2 (1969) 89.
[11] W. Łasocha, K. Lewiński, J. Appl. Crystallogr. 27 (1994) 437.
[12] T. Yamaguchi, O. Lindqvist, Acta Chem. Scand. A 35 (1981) 811.
[13] R. Eßmann, J. Mol. Struct. 356 (1995) 201.
[14] B. Hunter, Rietica—a visual Rietveld program, International Union of Crystallography on Powder Diffraction Newsletter No. 20 (Summer), 1998, http://www.rietica.org.
[15] A. Le Bail, H. Duroy, J.L. Fourquet, Mater. Res. Bull. 23 (1988) 447.
[16] S.W. Losvesey, T. Springer, (Eds.), Dynamics of Solids and Liquids by Neutron Scattering, Topics in Current Physics, Vol. 3, Springer, Berlin, 1977.
[17] E.R. Andrew, Nuclear Magnetic Resonance, Cambridge University Press, Cambridge, 1955.
[18] J.H. van Vleck, Phys. Rev. 74 (1948) 1168.
[19] G.W. Smith, J. Chem. Phys. 36 (1962) 3081.
[20] G.W. Smith, J. Chem. Phys. 42 (1965) 4229.
[21] G.W. Smith, J. Chem. Phys. 50 (1969) 3595.
[22] O. Kirstein, M. Prager, J. Combert, M.R. Johnson, Mol. Phys. Rep. 31 (2001) 47.
[23] R. Eßmann, P. Fischer, T. Vogt, Z. Anorg. Allg. Chem. 622 (1996) 597.
[24] N. Bloembergen, E.M. Purcell, R.V. Pound, Phys. Rev. 73 (1948) 679.
[25] J.S. Waugh, E.I. Fedin, Sov. Phys. Solid State 4 (1963) 1633.
[26] S.F. Sagnowski, S.A. Hodorowicz, B. Borzęcka-Prokop, Phys. Stat. Sol. A 107 (1988) 347.
[27] F. Altorfer, R. Essmann, Physica B 234–236 (1997) 61.
[28] N. Piślewski, J. Stankowski, L. Laryś, Phys. Stat. Sol. A 31 (1975) 415.